J. Fluid Mech. (1994), *vol.* 260, *pp.* 333–350

Statically unstable layers produced by overturning internal gravity waves

By S. A. THORPE

Department of Oceanography, The University, Southampton SO9 5NH, UK

(Received 23 February 1993 and in revised form 18 August 1993)

Internal waves in a uniformly stratified fluid of sufficiently large amplitude develop tilted layers in which the fluid is statically unstable. To investigate the evolution and subsequent development of this structure, experiments are made in which a horizontal rectangular tube containing a fluid of uniform density gradient is gently rocked at a selected frequency about a horizontal axis normal to the tube length. Large-amplitude standing internal gravity waves of the first mode are generated, and these steepen and overturn, the isopycnal surfaces folding to produce a vertically thin and horizontally extensive layer in which the fluid is statically unstable. In experiments with relatively small forcing, the layer persists for some 6 buoyancy periods, with no detected evidence of secondary instability, and static stability is re-established as the periodic flow reverses. The layer however breaks down, with consequent diapycnal mixing, when greater forcing is applied.

The scale and growth rates of instability in the overturning internal gravity waves are estimated using the theory developed in a companion paper by Thorpe (1994*a*). For the parameters of the laboratory experiments with relatively small forcing, the growth rates are small, consistent with the absence of signs of secondary instability. Larger growth rates and disturbance amplification factors of about 70 are predicted for the conditions in the experiment in which mixing was observed to occur. The experimental observations are consistent with an instability having a longitudinal structure.

We conclude that the form and development of breaking in internal gravity waves will vary according to the circumstances in which waves break, but depend on the Prandtl number of the fluid and, in particular, on the Rayleigh and Reynolds numbers of regions of static instability which develop as the waves overturn.

1. Introduction

1.1. *Background; breaking internal waves*

The breaking of internal gravity waves is a fundamental process contributing to turbulence in stratified fluids, and is an important mechanism of diapycnal mixing or of heat and momentum transport in the atmosphere and oceans. The nature of breaking and the subsequent transition stages, which eventually result in turbulent transfer, are however not fully understood. As a result of field and, especially, laboratory studies, several processes are known to play their part in particular circumstances. A helpful discussion of the concept of wave breaking is given by McIntyre & Palmer (1984, 1985), and some aspects of its dynamical consequences are addressed by McEwan (1983*a*, *b*).

Kelvin–Helmholtz (K–H) or Holmboe instability may be induced by fluid motion at the crest or trough of internal waves propagating on thin interfaces, such as those

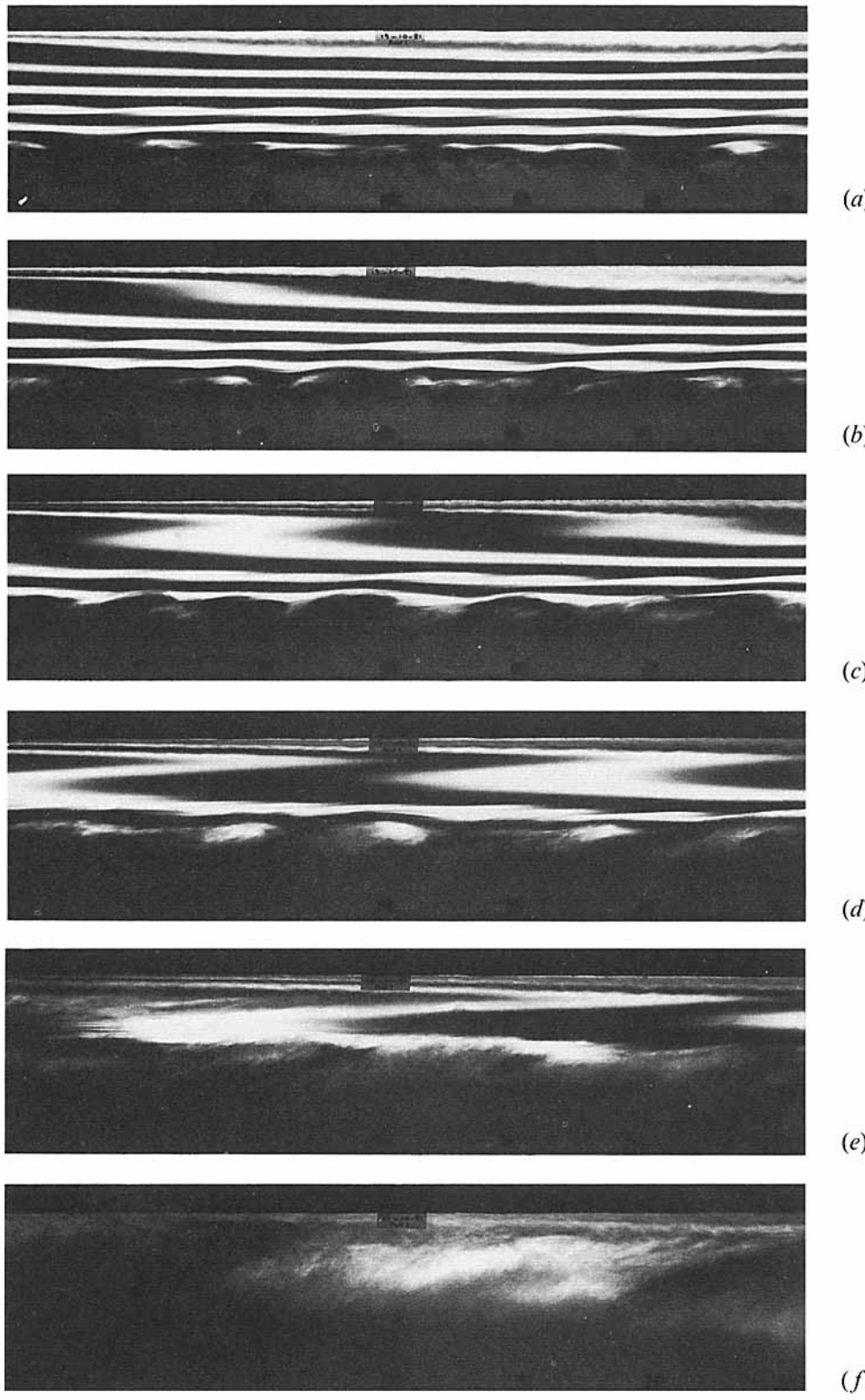

FIGURE 1. For caption see facing page.

found in the ocean thermocline (Woods 1968), with the generation of overturning billows. When a significant (ambient) shear is present, the crest or trough of an interfacial wave may steepen and overturn, forming a z-shaped pattern of isopycnals which includes regions of static instability, and this may precede the onset of K–H instability (Thorpe 1978*a*). A similar localized overturn (in contrast to the periodic overturns in K–H instability) of isopycnal surfaces occurs at the node of steep interfacial standing waves (Thorpe 1968*a*). The formation of z-shaped isopycnals appears to be a common feature of steep internal waves, being found in internal waves in uniformly accelerating shear flows (Thorpe 1978*b*, e.g. figures 5*g* and 7*h*), and in internal surges propagating from the ends of tubes filled with stratified fluids, when they are tilted to produce a shear flow. Examples of the latter are given in the series of photographs shown in figure 1. The presence and development of z-shaped structures in the surges propagating from the left-hand end of the tube can be seen near its upper boundary. These surges are presently the subject of investigation of Mrs S. Bruno in the Centre for Water Research at the University of Western Australia (private communication). The existence of waves containing regions of statically unstable stratification suggests that the selection of a condition in which isopycnals become vertical as a limit for the finite-amplitude evolution of internal waves (see for example Blumen 1988), may be arbitrary and unrealistic. The persistence and survival of such statically unstable overturning regions is a major subject of later discussion.

There are other ways in which internal waves break. One is by the formation of rotors, for example in solitary waves on density interfaces (Davis & Acrivos 1967), or in large-amplitude lee waves produced by flow over topography (Castro, Snyder & Marsh 1983; Rottman & Smith 1989), where the onset of rotor formation or wave breaking may be associated with an enhancement of wave drag (Miranda & James 1992), but the transitional stages leading to the formation of rotors, and the associated mixing within them, have received little attention.

Static instability on the scale of the waves has been observed in laboratory internal waves propagating vertically towards a critical layer (Thorpe 1981). Koop & McGee (1986) find K–H instability to develop in the non-uniform density, and velocity, gradient fields of waves with large vertical wavenumbers close to critical layers. Winters & D'Asaro (1989) simulate the development of density overturns by a two-dimensional numerical model of waves approaching a critical layer, which subsequently become unstable by a shear flow instability. In a related study, Winters & Riley (1992) choose to consider a simplified model. They examined the three-dimensional stability of a flow, $U = U_0 \cos z$, with density proportional to $\frac{1}{2}B \sin 2z + z(B-1)$, chosen to represent the velocity and density fields in waves approaching a critical layer, where B and U_0 are constants and z is the scaled upward vertical coordinate. For $0 \leqslant B \leqslant \frac{1}{2}$, the density is statically stable for all z, whilst for $\frac{1}{2} < B < 1$, the stratification varies in the vertical between statically unstable and stable values, but is stable at levels where the shear is greatest. Analytical solutions are found for the inviscid flow, and numerical solutions

FIGURE 1. Static instability with z-shaped isopycnals developing in a surge produced from an end of the tilted tube, 10 cm wide, 16 cm high and 4.82 m long, filled with stratified salt solution with a uniform density gradient. A turbulent region has been produced by flow over a regular array of bars fixed to the base of the tube. The buoyancy frequency is 2.55 s^{-1} and a shear flow has been produced by tilting the tube down on the left through an angle of 15.2° for 2.47 s before returning it to the horizontal. Photographs are shown at times of (*a*) 8.2 s; (*b*) 9.26 s; (*c*) 10.33 s; (*d*) 11.39 s, clearly showing the z-shaped overturn; (*e*) 12.46 s and (*f*) 13.52 s after the tube was returned to the horizontal. The photograph (*b*) is the last shown in the montage of photographs in figure 2(*b*) of Thorpe (1984), where further details are given.

are obtained for viscous and diffusive flow at a Reynolds number, $Re = 10^6$ and $B = 1$, when the density varies sinusoidally with z. (The stability of a similar density profile for $U_0 = 0$ is studied by Batchelor & Nitsche 1991, and their analysis and conclusions are described in the companion paper, Thorpe 1994*a*.) Although present in the inviscid analysis, no unstable modes are found at selected values of shear and wavenumber when the latter are taken to be in the flow direction; the presence of strong shear apparently completely inhibited any convective instabilities with such wavenumbers. Disturbances with cross-flow-directed wavenumbers, corresponding to longitudinal rolls, are however found that are unstable, pointing to the care needed to include consideration of three-dimensional disturbances in numerical simulations of the evolution of large-amplitude waves. Lin *et al.* (1993) also conduct numerical experiments to examine the nature of secondary instability following conditions of static instability when waves in a uniform density gradient approach a critical layer in a jet-like mean flow. Simulation at various values of the parameters indicate again that a Rayleigh–Taylor instability with longitudinal rolls is the most likely unstable secondary mode.

Conditions of static instability are also observed to develop in standing internal waves in a uniform density gradient in a rectangular container (Thorpe 1968*a*; McEwan 1971; Taylor 1992). McEwan (1971, 1973) describes the onset of 'traumata', regions of small-scale turbulence, in standing waves or in resonantly interacting internal wave trains, but offers no complete description of the processes leading to these conditions. Taylor (1992), however, shows that a variety of transient structures occur in forced standing waves, including interleaving (similar to the z-shaped folded isopycnals described above) and patterns resembling rising thermals and single rollers (his figures 1 and 2, respectively), suggesting that several processes may contribute to mixing, but defines no hierarchy or sequence of processes. One particular process of importance has however been identified; even small-amplitude internal waves in a uniform density gradient are prone to parametric instability (McEwan & Robinson 1975; Mied 1976; Drazin 1977; Klostermeyer 1982), but whilst this is suggested as a means to cascade energy to lower frequencies and to higher wavenumbers, the precise role of the instability in mixing is far from clear.

Steep, or breaking, internal waves are predicted as a consequence of interaction with inertial waves (Broutman 1984, 1986) or with larger scale waves (Thorpe 1989) in conditions favouring the development of wave 'caustics', where the group velocity of the internal waves matches the phase speed of the lower frequency, or longer, wave. The steepening and overturn of internal waves on reflection from sloping boundaries has been considered by several authors, particularly in connection with the resulting contribution to ocean boundary mixing (see for example Wunsch 1969; Thorpe 1987; Ivey & Nokes 1989), but with little attention being given to the transitional processes which lead to turbulence. The propagation through a fluid of a region where breaking is produced and carried by the velocity characteristics of both waves and wave groups, and the repetition frequency of breaking, are discussed by Thorpe (1988). The locus of extreme conditions, such as the minimum Richardson number, maximum shear or greatest wave slope, is predicted to be horizontal, with a recurrence period equal to the period of the internal waves.

We find, in the experiments described below, circumstances in which wave overturning occurs and persists for some finite period of time. If these conditions are 'supercritical', allowing infinitesimal disturbances to grow, and are sustained for a sufficient period of time to allow disturbances to achieve a substantial amplitude, then irreversible changes to the periodic flow and density field are expected, resulting in

appreciable energy dissipation, or at least in a redistribution of energy to different wavenumbers and frequencies. An objective of this study is to define more closely what these 'supercritical' conditions may be, and to begin an investigation of the nature of the disturbances that will gain energy as a result of the wave breaking. As a first step, we describe the static instability that may occur in standing or progressive waves in a uniform density gradient, and this provides an introduction to the experiments and their interpretation.

1.2. *Internal waves of finite amplitude in a uniform density gradient*

In fortunate contrast to surface gravity waves, there is an exact analytical solution of the fully nonlinear equations of motion that describe two-dimensional internal gravity waves in a fluid of constant density gradient, provided the effects of viscosity and diffusion may be neglected and conditions for the Boussinesq approximation are satisfied. These solutions for progressive and standing waves remain valid even when regions of static instability occur in the waves.

The solution for the stream function, ψ, and the non-dimensional density perturbation, ρ, of progressive waves is

$$\psi = (a\sigma/k)\sin(kx+mz-\sigma t), \tag{1}$$

$$\rho = (N^2 a/g)\sin(kx+mz-\sigma t), \tag{2}$$

where a is the wave amplitude, x and z the horizontal and vertical coordinates respectively, (k, m) the corresponding wavenumber vector, and g is the acceleration due to gravity. The x and z velocity components are given by $u = \partial\psi/\partial z$ and $w = -\partial\psi/\partial x$, respectively. The wave frequency, σ, is given by

$$\sigma^2 = N^2k^2/(k^2+m^2) = N^2\sin^2\Theta, \tag{3}$$

where N is the buoyancy frequency and Θ is the slope of the constant-phase surfaces. These surfaces are parallel to the direction of the wave group velocity and the motion of fluid particles, and normal to the phase speed vector. The fluid density is $\rho_0[1-(N^2/g)z+\rho]$ and its vertical gradient is zero when

$$am\cos(kx+mz-\sigma t) = 1, \tag{4}$$

that is on the constant phase line

$$kx+mz-\sigma t = \cos^{-1}(am)^{-1}. \tag{5}$$

The condition for the existence of regions of static instability is $am > 1$.

A corresponding exact solution for standing internal waves is

$$\psi = (a\sigma/k)\cos(kx+mz)\cos\sigma t, \tag{6}$$

$$\rho = (N^2 a/g)\sin(kx+mz)\sin\sigma t, \tag{7}$$

with static instability where

$$am\cos(kx+mz)\sin\sigma t > 1. \tag{8}$$

Again am must exceed unity for this condition to be satisfied somewhere in the fluid.

The shape of isopycnal surfaces $z = z_0+\zeta(x,t)$, where z_0 is the level of the isopycnal surface of density $\rho_0[1-(N^2/g)z_0]$ in the fluid in the absence of waves, ζ is given by the equation

$$\zeta = (g/N^2)\rho(x, z_0+\zeta, t) \tag{9}$$

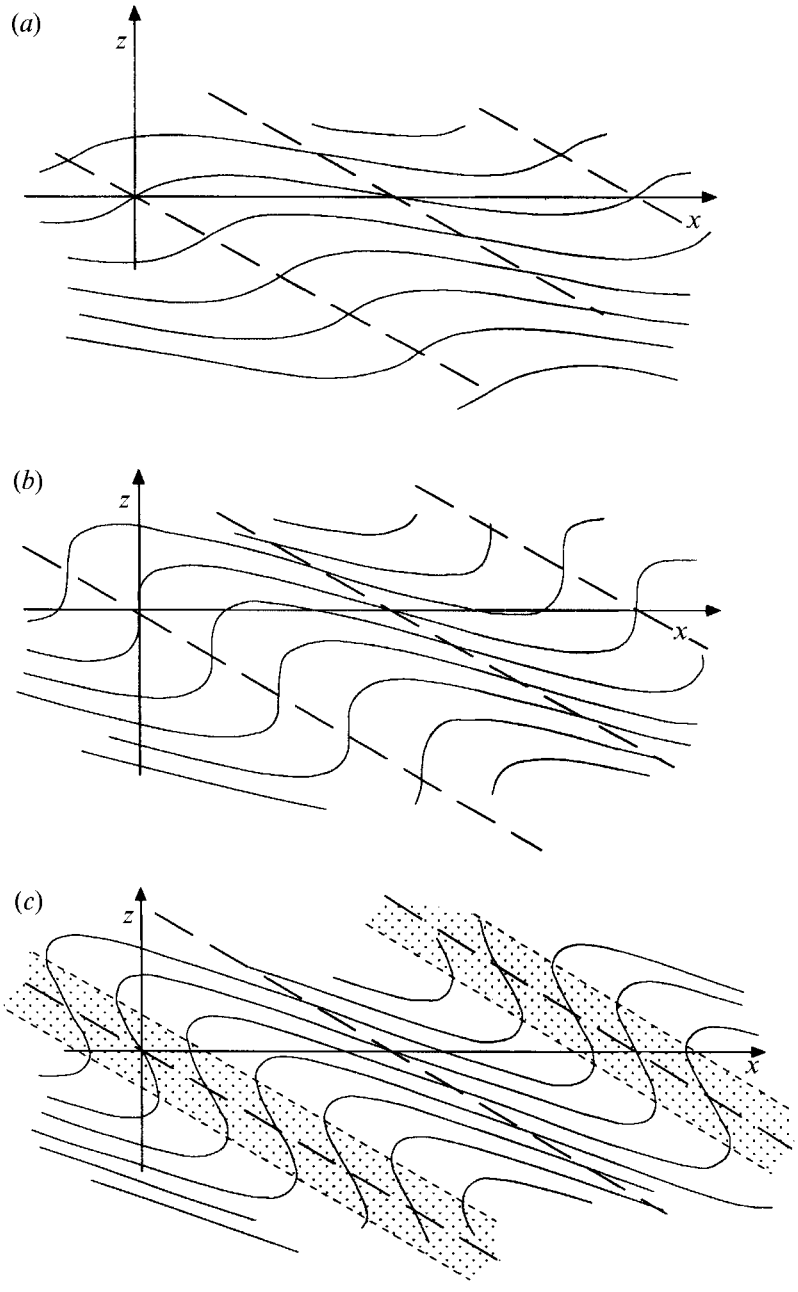

FIGURE 2. The form of isopycnal surfaces in two-dimensional internal gravity waves in a uniform density gradient. The propagation angle $\Theta = 30°$. (*a*) $am = 0.5$; (*b*) $am = 1.0$, incipient static instability; (*c*) $am = 1.5$, with regions of static instability shaded.

(see for example Thorpe 1968*b*). For progressive waves and without loss of generality, we take $z_0 = 0$ and $t = 0$, to obtain the shape of isopycnal surfaces

$$\zeta = a \sin(kx + m\zeta). \tag{10}$$

Figure 2 shows the shape of isopycnal surfaces for $\Theta = 30°$ in three cases: with no regions of static instability, with isopycnals which just become vertical, and with

regions of static instability that extend in relatively thin repetitive layers through the fluid. We obtain the same equation for standing waves at $z_0 = 0$ and at times $t = (2n+1)\pi/2\sigma, n = 1, 2, 3, \ldots$, when the fluid is at rest and the displacement is greatest, and at times of maximum displacement the density field of the finite-amplitude waves is given by

$$\rho_1 = \rho_0\{1-(N^2/g)[z+a\sin(kx+mz)]\}. \tag{11}$$

At these times the density and isopycnal distributions are identical for progressive and standing waves. In progressive waves, however, the regions of static instability shown in figure 2(*c*) propagate through the fluid at the wave phase speed $\sigma/(k^2+m^2)^{\frac{1}{2}}$ in a direction normal to the constant-phase surfaces, whilst in standing waves the regions of static instability persist for only a period short in comparison to the wave period. If, however, wave breaking derives from a Rayleigh–Taylor instability developing in the regions of static instability, and has constant phase-lines parallel to the flow so that the fluid motion induced by the wave plays no part (see Thorpe 1994*a*), and if the instability has an inverse growth rate that is small in comparison to the period of time for which the conditions of static instability in the wave field are maintained, then the form of breaking in progressive and standing waves will be similar. A study of one or other may lead to information of more general application.

For practical reasons we choose to focus attention on standing waves. These are readily forced to large amplitude in the laboratory. It is, naturally, impossible to reproduce the conditions of the infinite fluid in which the above solution is valid, but approximate solutions are available to describe the density and velocity fields in a rectangular container with horizontal and vertical boundaries. These solutions are described in §2.1 and, although unable to predict the conditions or regions of wave overturn, indicate those in which steep isopycnals will occur, the precursors of static instability. Experiments made in a long rectangular tube are described in §2.2. They show that, as indicated by the solutions, static instability occurs in horizontally extensive, but vertically shallow, layers and persists for periods of several times the buoyancy period of the fluid, with evidence of secondary instability when the forcing is sufficiently large.

If $k \ll m$, as is common in the ocean, the horizontal density gradients are much less than the vertical ones, and the local density field perturbed by internal waves (11) is approximately uniform in the horizontal. Locally it may be written

$$\rho_1 = \rho_0[1-(N^2/g)z + A\sin Kz], \tag{12}$$

where A is a constant ($\ll 1$) and $K(=m)$ is the vertical wavenumber. This local density field will determine the conditions for instability of the waves, provided at least that the aspect ratio of the evolving instability is large in comparison to that of the density field and the growth rate of the instability is large in comparison to the evolution rates of the disturbed fields of density and velocity in the internal waves. This x-independent density profile with layers of static instability separated by layers of enhanced stability (buoyancy frequency $> N$) has been discussed by Thorpe (1994*a*) and provides a good description of the density field in the laboratory experiments. It is therefore used to help explain the presence or absence of detected secondary instability in the experiments.

2. Standing internal gravity waves in a rectangular container with a uniform density gradient

2.1. *Theory*

Thorpe (1968*a*) described a technique to derive a Stokes-like expansion for standing internal gravity waves in a rectangular container of length, L, and depth, H, when the Boussinesq approximation is valid. Taking horizontal and vertical axes x, z at one corner of the container and wavenumber vector (k, m), the solutions to second order are

$$\psi = (a\sigma_0/k)\sin kx \sin mz \sin \sigma t \tag{13}$$

for the stream function, with density

$$\rho_1 = \rho_0[1 - \left(\frac{N^2}{g}\right)(z - a\cos kx \sin mz \cos \sigma t + \tfrac{1}{8}a^2 m \sin 2mz(1 + \cos 2\sigma t))], \tag{14}$$

where the wave frequency is $\sigma = \sigma_0$ with

$$\sigma_0^2 = (N^2k^2)/(k^2 + m^2). \tag{15}$$

We may determine the region of small negative or of positive (statically unstable) density gradients by defining the locus of points on which the density gradient reaches a specified value, QN^2/g, where Q is a non-dimensional constant, positive in unstably stratified regions. To second order we find

$$Q = -1 + am\cos kx \cos mz \cos \sigma t - (\tfrac{1}{2}am)^2 \cos 2mz(1 + \cos 2\sigma t) \tag{16}$$

which, referred to axes x', z' at the centre of the container and limiting attention to the first internal wave mode, can be written

$$Q + 1 = am \sin kx' \sin mz' \cos \sigma t + (\tfrac{1}{2}am)^2 \cos 2mz'(1 + \cos 2\sigma t),$$

where now $k = \pi/L$ and $m = \pi/H$. Writing $X = \sin kx$ and $Z = am \sin mz'$, and choosing $t = 0$, the time of maximum density perturbation, we have

$$Z^2 - XZ + Q + 1 - \tfrac{1}{2}(am)^2 = 0, \tag{17}$$

which is a hyperbola with asymptotes $X = Z$ and $Z = 0$. If $(am)^2 < 2(1 + Q)$, the hyperbola has no real values of Z at $X = 0$ and, for $X > 0$, lies in the sector between $X = Z$ and $Z = 0$. The region in which the density gradient exceeds Q does not then extend to the centre of the container. The hyperbola intersects the Z-axis at $Z = \pm[\tfrac{1}{2}(am)^2 - Q - 1]^{\frac{1}{2}}$ when $(am)^2 > 2(1 + Q)$. Real values for Z at the tube ends can only be found if (16) has real roots at $x = t = 0$, when

$$(am)^2 > \tfrac{3}{2} + 2Q. \tag{18}$$

In summary, at second order, no surfaces of constant density gradient, Q, exist if $(am)^2 < \tfrac{3}{2} + 2Q$. When $2 + 2Q > (am)^2 > \tfrac{3}{2} + 2Q$, this gradient is reached on (and exceeded within) surfaces which do not extend to the centre of the container. When $(am)^2 > \tfrac{3}{2} + 2Q$, the region in which the specified density gradient is reached and exceeded extends along the whole tube, the shape near the centre (small kx and mz) being approximately hyperbolic with asymptotes $z = 0$ and $z = kx/(am^2)$. In the experiments to be described in §2.2, am is of order unity and $m \gg k$, and the prediction of this second-order analysis is that the central axis of the high-gradient region, bisecting the asymptotes, is tilted at an angle of approximately $(\sqrt{2} - 1)k/(am^2)$ or approximately $0.414H/(amL)$ to the horizontal.

The second-order approximation is, however, found to be valid only for sufficiently small values of am. We have continued the expansion to fourth order.† Decrease in the

† Copies of the expressions for density perturbations may be obtained from the editor or author.

magnitude of successive terms in ψ and its first derivatives, the velocity components, is rapid. The horizontal flow near the centre of the container is approximately sinusoidal in z with wavenumber K, even when am is of order unity. This implies that, to the extent to which the limited series can provide a useful prediction, the horizontal velocity of, and near, the layer in which static instability is found in the experiment described in §2.2, varies approximately linearly with z, and that the shear is therefore uniform. This conclusion will be used in §3 when we come to estimate the growth rates of disturbances. The vertical density gradient is, however, strongly influenced by higher-order terms, particularly those at fourth order which are solely functions of z and t. We have calculated the size of terms at each order contributing to the density gradient when it first reaches the non-dimensional value Q at $x = 0$, and the corresponding 'slope', am. In each case the time at which the maximum gradient was reached was $t = 0$. The results are shown in figure 3. Although, for $Q < -0.4$, third- and fourth-order terms are less than 20% of the leading terms, signs that the series is convergent are at best weak, and as Q approaches zero (corresponding to the onset of static instability), the higher-order terms significantly become large and even the truncated series does not suggest convergence.

It follows that precise definition of the conditions of the onset of static instability cannot be established by the second- or fourth-order expansions alone, and requires a new approach, perhaps by an efficient means of calculating higher-order terms or by numerical computation. It appears likely however that a 'slope', am, of about unity is necessary to promote conditions of static instability, that the horizontal flow has a vertical structure that is only slightly modified by terms of order higher than the first, remaining approximately sinusoidal in z when am is of order unity, and that, in the centre of the container, instability will first be approached in a layer of small vertical and relatively large horizontal extent.

2.2. *The laboratory experiments*

Standing internal waves were generated by rocking a Perspex tube, filled with a stratified salt solution, about a horizontal axis. The tube is 295 cm long, 10 cm deep and 26.1 cm wide. It was filled whilst vertical, using the standard two-tank technique with water and brine, to produce a uniform density gradient. Small quantities of dye were injected into the inlet tube during filling to mark isopycnal surfaces. Once completely full, with all the air removed, the tube was slowly and carefully (to avoid mixing) rotated into a horizontal position, thus stretching and thinning the dye bands. One end of the tube was then connected by a near-vertical rigid shaft to the eccentric drive of a motor and gear box with preset amplitude and frequency chosen to match that of the first internal wave mode.

The buoyancy frequency in the experimental runs was between 2.37 and 2.69 rad s^{-1}, with corresponding first mode wave frequencies of 68.9–78.2 s. The chosen forcing frequencies were within 3% of the natural frequencies of the first internal wave mode. The amplitude of the forcing (half the angle of oscillation) was adjusted between runs in the range 3.7×10^{-3} to 8.8×10^{-3} rad. All experiments were begun with the tube horizontal at the mid-point of the drive stroke. The motor was then switched on, causing an initial downward motion of the right-hand end of the tube. The response of the fluid was such that after three-quarters of a cycle, and at each successive half-cycle, the isopycnals became horizontal, or nearly so, at least until onset of irregular motion. Maximum displacements occurred at times close to each half-cycle of the motor drive measured from its start. Visual observations were made of the shape and motion of the dye layers. Several experiments were recorded on video. Photographs

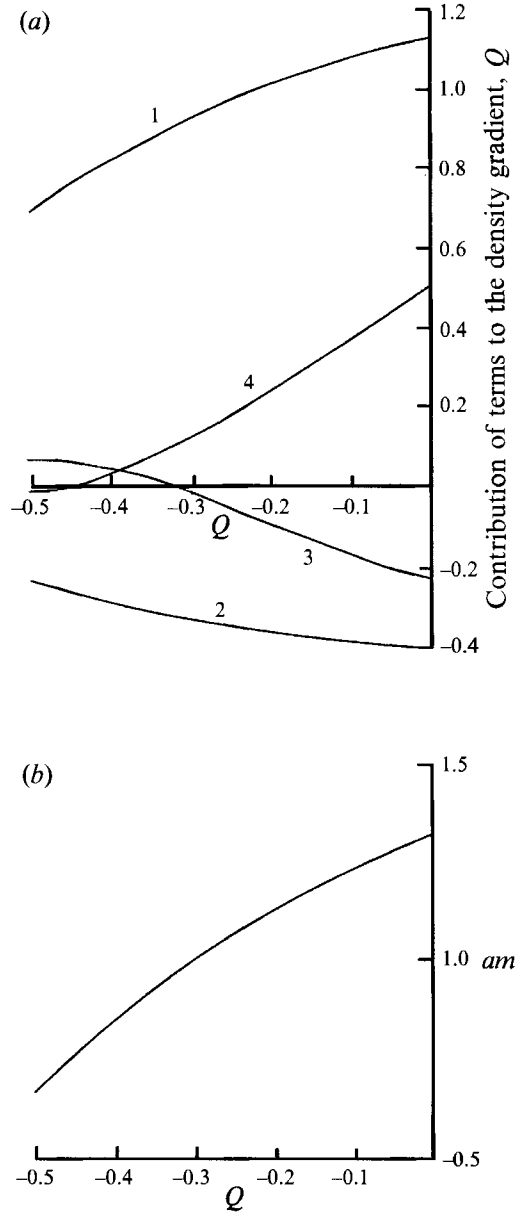

FIGURE 3. (*a*) The size of terms of order one to four in the fourth-order expansion for the density gradient at the point in a standing wave where the maximum density gradient is reached, as functions of the maximum non-dimensional gradient, Q. Here the aspect ratio of the wave mode, k/m, is equal to 0.01. The values are, however, insensitive to a variation in k/m to 0.1, and change by less than 5% at $k/m = 1$. (*b*) The 'slope', am, of standing internal waves as a function of the maximum non-dimensional density gradient, Q, using the fourth-order expansion for the waves. The 'slope' required to produce zero gradient in the first-order solution is $am = 1$.

were taken at regular, and, when appropriate, at irregular, intervals, viewing the tube horizontally and also vertically near the centre and at one end, and using shadowgraphs to display the horizontal planform of any disturbances which might evolve.

Figure 4 shows (*a*) the initial pattern of dye layers before oscillation, and the wave

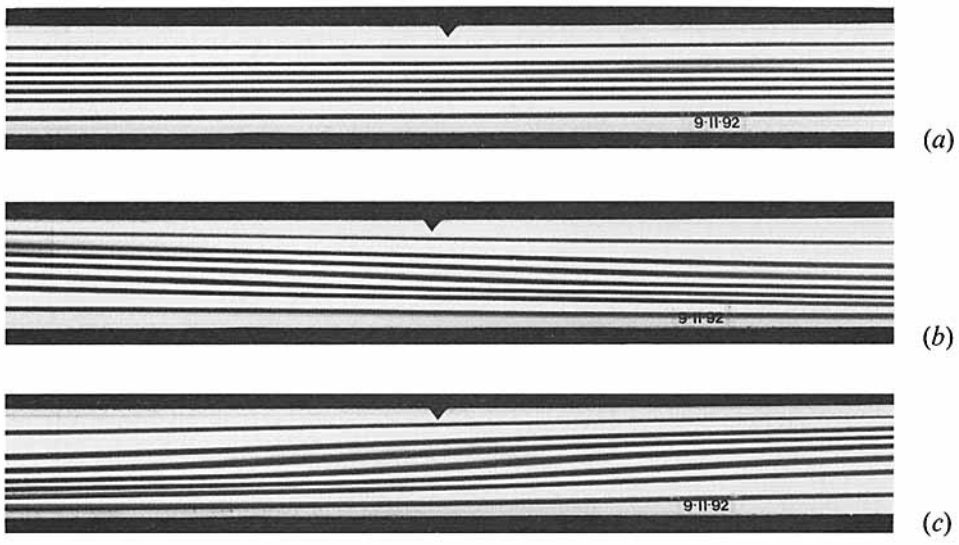

FIGURE 4. The form of standing internal waves near the centre of a tube (marked at the top by a triangle) of height 10 cm with $N = 2.37\ \text{s}^{-1}$. The tube is rocked about a horizontal axis 23.5 cm below the centre of the tube at a frequency of $7.85 \times 10^{-2}\ \text{s}^{-1}$. The natural frequency of the first mode is $8.03 \times 10^{-2}\ \text{s}^{-1}$. Photograph (*a*) was taken before the motion was started, the horizontal lines are bands of dye marking isopycnals; (*b*), (*c*) show the form of waves at maximum displacement when the tube is rocked through an angle of 3.73×10^{-3} rad.

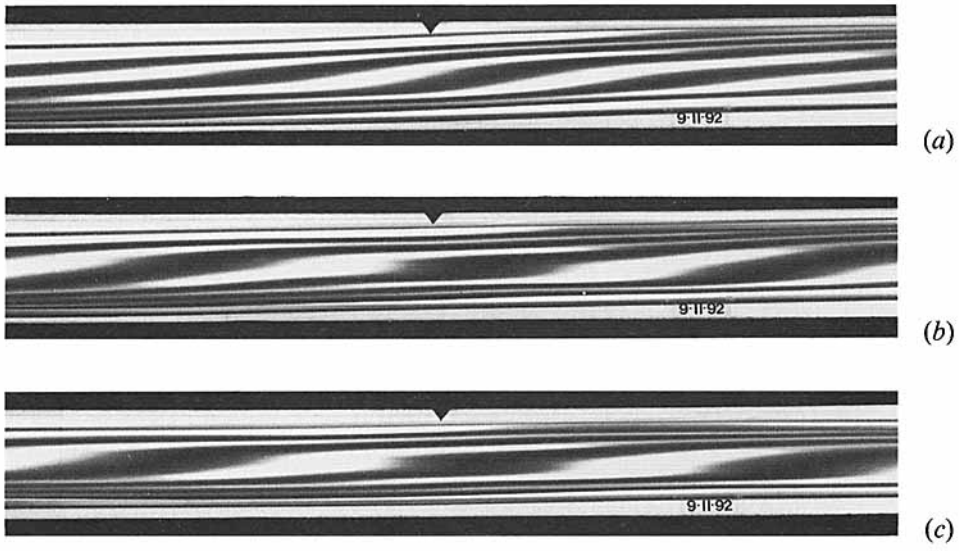

FIGURE 5. As in figure 4, but showing the development of static instability when the tube amplitude is 6.1×10^{-3} rad. The photographs (*a–c*) are about 3 s apart and are taken after $2\frac{1}{2}$ tube oscillations.

form near the centre of the tube at a time close to its maximum amplitude for a forcing amplitude of 3.63×10^{-3} rad and after (*b*) $4\frac{1}{2}$, and (*c*) 5 cycles of forcing. The tube is close to horizontal at this time with the left-hand end rising. No signs of small-scale disturbances or of wave breaking are visible. Figure 5 shows the onset of isopycnal overturn near the centre of the tube with enhanced forcing, 6.10×10^{-3} rad. The tube is again horizontal with the left-hand end rising. The displacement amplitude of the

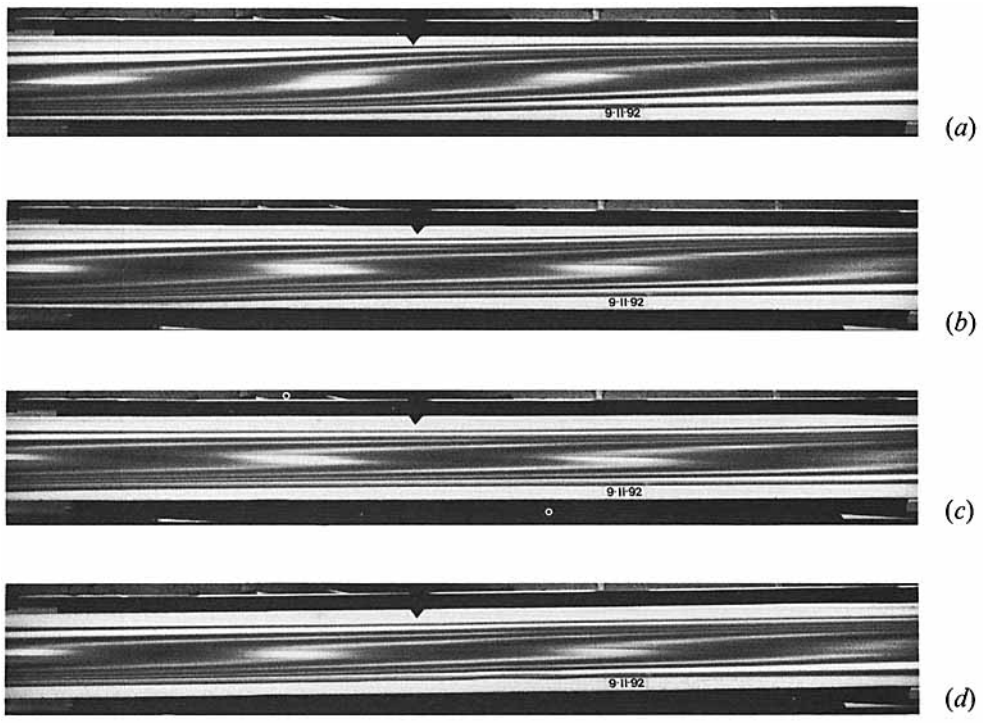

FIGURE 6. As in figure 4, but showing the development of static instability when the tube amplitude is 8.14×10^{-3} rad and after $1\frac{1}{2}$ tube oscillations. The dye lines and their overturning are best seen by viewing the photographs at a low angle from one end.

isopycnal at the end of the tube is approximately 3.0 cm, giving $am = 0.95 \pm 0.1$. The isopycnal surfaces near mid-depth steepen, the dye bands there becoming thicker and more diffuse but with no sign of small-scale mixing, and then overturn forming a z-like structure similar to those shown in figure 1. Static instability occurs over a vertical scale of about 1 cm and individual isopycnals fold over a maximum length of about 19 cm. The overturning region extends the full width of the photographs, 75 cm, has a small tilt of about 0.018 ± 0.002 (higher to the left) and persists for about 8 s before being removed by the reversing periodic flow of the standing wave. The tilt compares with the estimates of second-order theory (§2.1) of 0.015 ± 0.002, and has the same sense in respect to the wave phase. The overturning structure is seen more clearly in figure 6, where the drive amplitude has been increased to 8.14×10^{-3} rad. The horizontal scale of the z-folds is now some 30 cm and they persist for 16 s, or 6 buoyancy periods. The subsequent motion, e,g. as shown in figure 7 one half-cycle after figure 6, becomes very irregular, particularly at each half-cycle when the wave steepness is greatest, with overturning reoccurring in the centre of the tube. There is evidence of solitary waves or wave trains propagating near the upper and lower boundaries (figure 7*b*, *c*), where the fluid has become turbulent and mixed, so providing a density structure that can support internal surges (Benjamin 1967).

The horizontal structure of the z-shaped overturning regions was examined by propagating a vertical columnated beam of light through the tube to produce shadowgraph images on tracing paper on the bottom of the tube. In view of the theory developed in Thorpe (1994*a*), it was expected that some evidence of secondary patterns evolving in the region of unstable stratification might be seen. The shadowgraphs

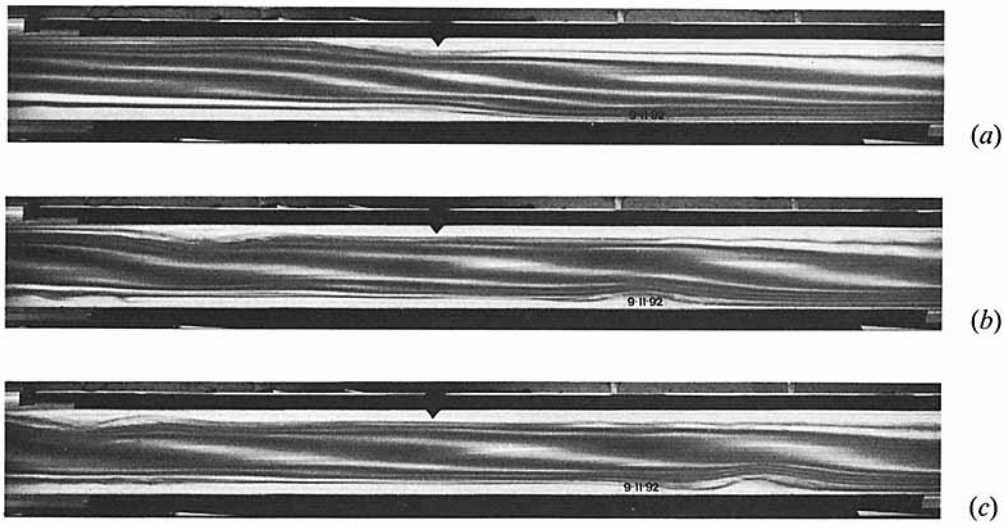

FIGURE 7. The development of irregular motion one half-cycle following figure 6. Photographs are about 4 s apart. Solitary waves can be seen propagating along the upper and lower boundaries of the tube.

proved sensitive to small changes in refractive index gradient produced by boundary mixing. No evidence of any coherent structure was observed however that could unambiguously be associated with the existence of the z-like overturns at times when they were visible; indeed no structure was seen that could not be associated either with the development of mixing at the sidewalls of the tube or, at a stage when the motion became disordered, with instability or waves in the boundary layers adjoining the horizontal boundaries.

Forcing was again increased to a drive amplitude of 8.81×10^{-3} rad. Figure 8 shows the evolution of the overturning region. In this case the z-pattern, rather than remaining distinct, collapsed at a time of about 10 s after the first onset of conditions of static instability, leading the changes visible in figure 8(*d*, *e*). There were, significantly, no signs of across-tube transverse eddies, and it is concluded that the secondary instability following static instability is not one with constant-phase lines parallel to the vorticity of the mean flow as, for example, in Kelvin–Helmholtz instability. The resulting mixing resulted in diapycnal diffusion, thickening the dyed layer. This is evident in comparing figures 8(*a*), before instability when the motion is steepening the isopycnal surfaces, and 8(*g*), when the flow field has reversed.

2.3. *Discussion*

Static instability was observed in a thin linear region, as in figure 2(*c*), of large horizontal extent and of height small in comparison to the tube depth. The observed tilt of the region is small and close to that predicted by the second-order theory of §2.1. It should be noted that, in order to avoid the effects of parametric instability (McEwan & Robinson 1975; see also Thorpe 1994*b*), the forcing was increased to such an extent that the standing waves overturned at a short time, only one and a half to three cycles after the onset of the tube motion (see figure captions) and that it is possible that the waves are not, at this time, independent of the initial conditions.

The statically unstable structures seen in the experiments are very similar to those already found elsewhere (e.g. in figure 1), and appear to be characteristic of progressive

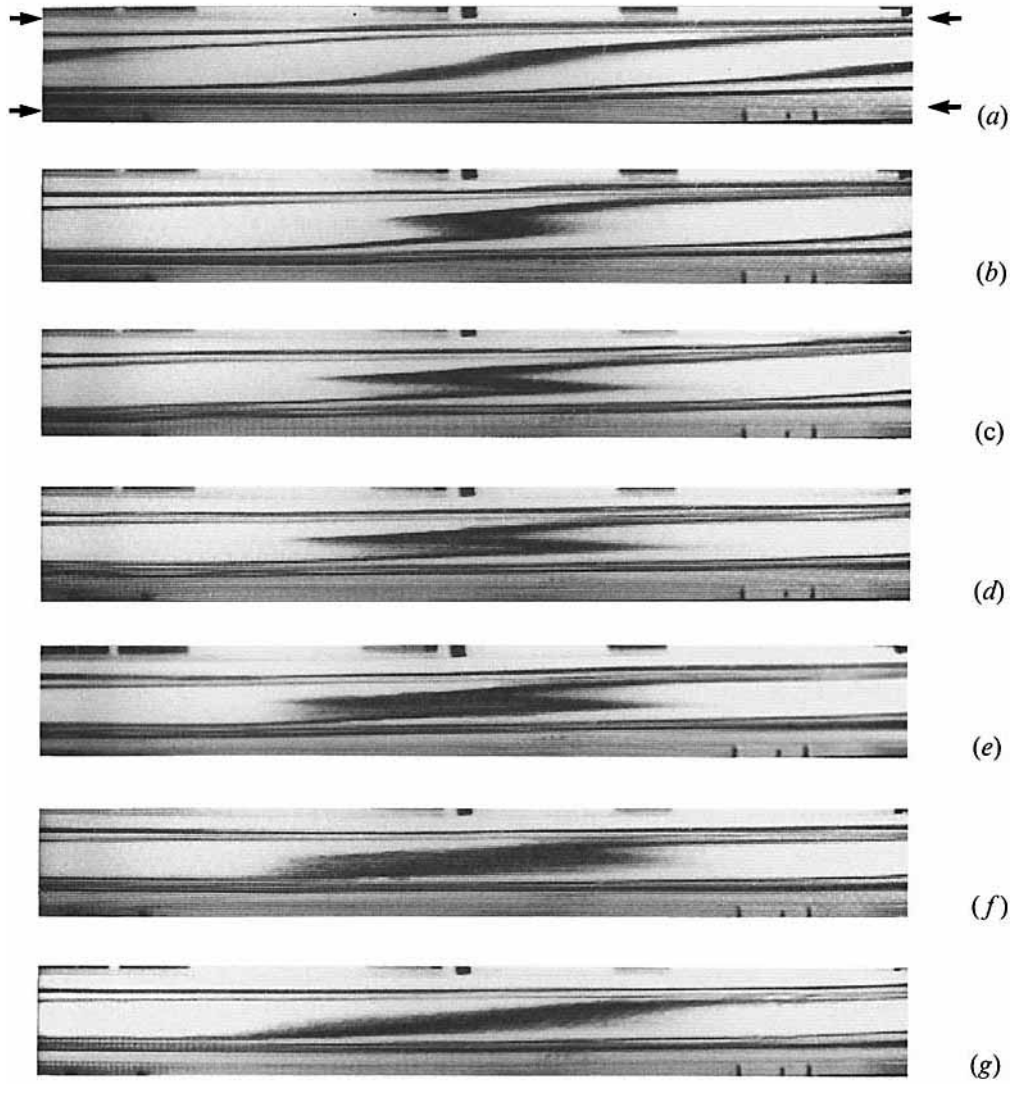

FIGURE 8. The development of static instability and mixing. Here $N = 2.57\ s^{-1}$ and the tube rocking frequency is $8.57 \times 10^{-2}\ s^{-1}$. The frequency of the first mode is $8.71 \times 10^{-2}\ s^{-1}$. Only five dye layers are present, of which that at mid-depth is most obvious in the photographs taken from a video and showing the tube $1\frac{1}{2}$ cycles after the start of oscillation. Photographs are shown at times after (*a*) 0, (*b*) 4 s, (*c*) 8 s, (*d*) 10 s, (*e*) 12 s, (*f*) 14 s, (*g*) 18 s. The arrows in (*a*) mark the levels of the top and bottom boundaries of the 10 cm deep Perspex tube. The central dye line and its mixing are best seen by viewing the photographs at a low angle from one end.

waves in shear flows where static instability precedes K–H instability, as well as of standing waves.

3. Discussion; the growth of disturbances in standing waves

A stability analysis of a fluid with density profile given by (12) which locally describes the density in the overturning waves in the experiments, is given by Thorpe (1994*a*). This predicts growth rates of disturbances which can be applied to the laboratory experiments. Growth rates depend on the Rayleigh, Prandtl, and Reynolds

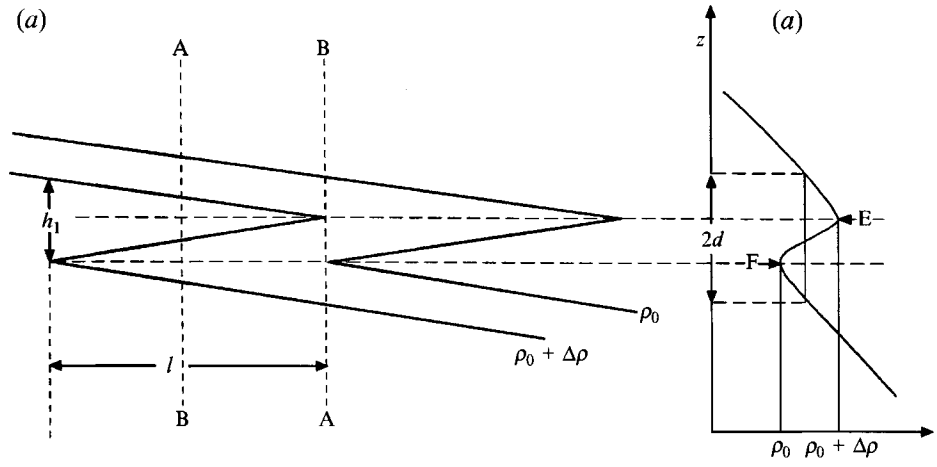

FIGURE 9. Definition sketch showing overturning isopycnal surfaces and corresponding scales referred to in the text: (*a*) isopycnals; (*b*) density profile.

numbers which characterize the flow and density fields, as well as on a parameter, r, equal to N^2/gKA, which describes the shape of the density profile (12). The Rayleigh number is given by $Ra = gB_1 d^4/\nu\mathscr{D}$, where $\rho_0 B_1$ is the density gradient at the centre of the statically unstable layer, d is the vertical scale of the overturning region as shown in figure 9, and ν and $\mathscr{D}$ are the kinematic viscosity and density molecular diffusivity, respectively. (Ra is equal to Ra_M in Thorpe 1994*a*). Pr is equal to $\nu/\mathscr{D}$, about 700 for the salt-stratified laboratory fluid, and $Re = U'd^2/\nu$, where U' is the vertical shear. Growth rates are estimated for fluids in which the shear in the region of density overturn is uniform as, to a first approximation, is the shear expected in the experiments (§2.1).

To use the predictions to obtain estimates of the laboratory growth rates, we must first estimate the Rayleigh number in the z-shaped isopycnal regions. The height, h_1, (figure 9) characterizes the vertical scale of the z-structure, and this may be equated to $2d$ from consideration of the vertical density profile at section BB. The height of the region of positive (statically unstable) density, EF, is approximately $\frac{1}{2}h_1$, so that the maximum density gradient is $2\Delta\rho/h_1$, where ρ_0 and $\rho_0 + \Delta\rho$ are the densities of the two isopycnals chosen so that their folded regions just reach section AA. The density difference, $\Delta\rho$, of the isopycnal surfaces may be calculated from the difference in density of dyed isopycnals in the experiment, $\Delta\rho_1$, and their observed horizontal separation, L_1; $\Delta\rho = l\Delta\rho_1/L_1$, where l is the isopycnal folding length. $\Delta\rho$ is found from the initial vertical separation of the dyed isopycnals, h; $\Delta\rho_1 = h\rho_0 N^2/g$. We may therefore estimate the Rayleigh number of the fluid in the z-shaped structure in terms of measurable quantities: $Ra = lhh_1^3 N^2/(8L_1\nu\mathscr{D})$.

The appropriate value of r may be estimated from d and the tube height, $H = 10$ cm. For example, in the experiment shown in figure 6, h_1 $(= 2d) = 0.8$ cm, so that $2d/H = 0.08$ and we find $r = 0.98$. We have $l = 30$ cm and $L_1 = 60$ cm, $h = 0.8$ cm and $N = 2.57\ \mathrm{s}^{-1}$, so that, with $\nu = 0.01\ \mathrm{cm\ s}^{-1}$ and $\mathscr{D} = 1.4 \times 10^{-5}\ \mathrm{cm}^2\ \mathrm{s}^{-1}$, we find $Ra = 1.51 \times 10^6$, with an estimated error of $\pm 0.4 \times 10^6$. This considerably exceeds the critical Rayleigh number, 88.0, and the fluid should therefore be unstable.

The corresponding maximum growth rate of the disturbance with wavenumber transverse to the flow is obtained from figure 5(*b*) of Thorpe (1994*a*) and converts into a dimensional value of $0.228\ \mathrm{s}^{-1}$. The non-dimensional wavenumber of the instability

is $\beta = 3.26$, corresponding to a wavelength $2\pi d/\beta$ of 0.77 cm, a scale sufficiently large to be detected in the shadowgraphs. If we take half the maximum growth rate as a best present estimate of the actual growth rate of a disturbance over the period, 16 s, for which the z-structure persists, then an infinitesimal disturbance would be amplified by a factor $\exp(16 \times 0.114) = 6.2$. This is not very large, and perhaps explains why no resulting disturbance is detectable. Caution is necessary for several reasons. For example, the timescale of growth of the disturbance is not much less than the evolution timescale of the density field, so that the assumption of a steady state is violated. The Reynolds number of the laboratory flow is 75 ± 15, obtained using an estimate of shear derived from the horizontal scale of the z-structure, 30 cm, produced in 8 s with a vertical scale $d = 0.4$ cm. The growth rate at these values of Ra and Re derived from a numerically derived equation (Thorpe 1994*a*, (32), §3.5) for the growth rates, but with considerable interpolation, is negative. This supports a hypothesis that the mode with transverse wavenumber, with positive growth rates as found above, will dominate.

For comparison, the experiment shown in figure 8 and in which mixing was observed, has $Ra = (6.94 \pm 1.8) \times 10^7$ and $r = 0.87$, corresponding to a dimensional growth rate of 0.42 s^{-1} and a disturbance amplification factor of 66.7 at the time instability was first seen. The absence of transverse structure in the transition from static instability is consistent with an instability having constant-phase lines parallel to the flow.

These conclusions are conditional on assumptions made in deriving the estimates of growth rates, of which that most likely to fail is that a linear description remains accurate at Rayleigh numbers that are far greater than the critical. The inverse growth rate in the final experiment described (figure 8) are much less than the wave periods and, more significantly, are much smaller than the times for which wave overturn persists, indicating that the steady-state assumptions are likely to be valid.

4. Conclusions

In the experiments on standing waves and in earlier experiments referred to in §1.1, thin elongated statically unstable layers are observed. The layers may persist for several times the overall buoyancy period. When instability is observed (figure 8), it does not have a transverse structure.

Comparison of the growth rates at similar Rayleigh numbers and scale of overturn (parameterized by r) using the theory developed by Thorpe (1994*a*), shows that the extensive horizontal regions of statically unstable fluid found in the experiments (figures 5 and 6) at $Pr = 700$ would be less likely to persist without the evolution of large secondary instabilities in thermally stratified ocean waters ($Pr \approx 7$) or in the atmosphere ($Pr \approx 0.7$), since the growth rates would be greater at comparable Rayleigh numbers. The development of turbulence in breaking internal waves may therefore depend on the Prandtl number of the fluid. The effects of shear on the stability of fluid that is unstably stratified will depend on the detailed flow structure (see again Thorpe 1994*a*), which may vary from one kind of breaking internal wave to another (§1.1). It appears unlikely that, without a careful analysis of the time development of the flow field and the variation of parameters (the Reynolds and Rayleigh numbers in particular) in the period following wave 'overturn' and during which disturbances are growing to measureable amplitude, the form of the dominant instability can be accurately predicted. The evolution, and hence the form of internal wave breaking, may differ in different circumstances, thus leading to a yet unclassified hierarchy of types of breaking waves, akin to the spilling and plunging classes of surface gravity

waves. It is possible that several modes may grow simultaneously at similar rates. Taylor's (1992) experiments on internal standing waves were in a range of slopes $0.89 < am < 1.2$ (private communication) in which isopycnal overturning appears likely, and the interleaving of density surfaces and the 'traumata' reported by McEwan (1973) may have been caused, in part, by the development of z-structures found here, whilst the variety of structures observed by Taylor supports the conjecture that several modes of instability may grow simultaneously. The contribution of parametric instability is, however, a further important contributing factor in these experiments (McEwan & Robinson 1975), and to some other types of breaking waves (Thorpe 1994*b*). In the natural environment, the generally larger scales of waves, motion and density structure may contribute to larger Rayleigh and Reynolds numbers than found in the laboratory, whilst enhanced levels of 'background' disturbance will contribute larger 'initial' disturbances, each increasing the likelihood that secondary instabilities will lead to turbulence and mixing.

It is important to note that the generation of the z-shaped regions of static instability in standing or progressive internal waves has not been explained. There are, moreover, no solutions available to describe the large-amplitude standing waves in a rectangular container (§2).

The experiments described above were made at the Centre for Water Research at the University of Western Australia during a period of study leave in 1992. I am grateful to Mr John Devill and Mr Bill Deugh for their expert construction of apparatus, to Mr Seng Giap Teoh, Mrs Silvia Bruno and to my wife, Daph, for their help in recording the experiments, and to the CWR and the Royal Society for financial support which made the very pleasant visit possible.

REFERENCES

BATCHELOR, G. K. & NITSCHE, J. M. 1991 Instability of stationary unbounded stratified fluid. *J. Fluid Mech.* **227**, 357–391.

BENJAMIN, T. B. 1967 Internal waves of permanent form in fluids of great depth. *J. Fluid Mech.* **29**, 559–592.

BLUMEN, W. 1988 Wave breaking in a compressible atmosphere. *Geophys. Astrophys. Fluid Dyn.* **43**, 311–332.

BROUTMAN, D. 1984 The focussing of short internal waves by an inertial wave. *Geophys. Astrophys. Fluid Dyn.* **30**, 199–225.

BROUTMAN, D. 1986 On internal wave caustics. *J. Phys. Oceanogr.* **16**, 1625–1635.

CASTRO, I. P., SNYDER, W. H. & MARSH, G. L. 1983 Stratified flow over three-dimensional ridges. *J. Fluid Mech.* **153**, 261–282.

DAVIS, R. E. & ACRIVOS, A. 1967 Solitary internal waves in deep water. *J. Fluid Mech.* **29**, 593–607.

DRAZIN, P. G. 1977 On the instability of an internal gravity wave. *Proc. R. Soc. Lond.* A **356**, 411–432.

IVEY, G. N. & NOKES, R. I. 1989 Vertical mixing due to the breaking of critical internal waves on sloping boundaries. *J. Fluid Mech.* **204**, 479–500.

KLOSTERMEYER, J. 1982 On parametric instabilities of finite-amplitude internal gravity waves. *J. Fluid Mech.* **119**, 367–377.

KOOP, C. G. & MCGEE, B. 1986 Measurements of internal gravity waves in a continuously stratified shear flow. *J. Fluid Mech.* **172**, 453–480.

LIN, C.-L., FERZIGER, J. H., KOSEFF, J. R. & MONISMITH, S. G. 1993 Simulation and stability of two-dimensional internal gravity waves in a stratified shear flow. *Dyn. Atmos. Oceans* (to appear).

MCEWAN, A. D. 1971 Degeneration of resonantly excited standing internal gravity waves. *J. Fluid Mech.* **50**, 431–448.

McEwan, A. D. 1973 Interactions between internal gravity waves and their traumatic effect on a continuous stratification. *Boundary-Layer Met.* **5**, 159–175.

McEwan, A. D. 1983*a* The kinematics of stratified mixing through internal wavebreaking. *J. Fluid Mech.* **128**, 47–57.

McEwan, A. D. 1983*b* Internal mixing in stratified fluids. *J. Fluid Mech.* **128**, 59–81.

McEwan, A. D. & Robinson, R. M. 1975 Parametric instability of internal gravity waves. *J. Fluid Mech.* **67**, 667–687.

McIntyre, M. E. & Palmer, T. N. 1984 The 'surf zone' in the stratosphere. *J. Atmos. Terr. Phys.* **46**, 825–849.

McIntyre, M. E. & Palmer, T. N. 1985 A note on the general concept of wave breaking for Rossby and gravity waves. *Pure Appl. Geophys.* **123**, 964–975.

Mied, R. P. 1976 The occurrence of parametric instability in finite-amplitude internal gravity waves. *J. Fluid Mech.* **78**, 763–784.

Miranda, P. M. A. & James, I. N. 1992 Non-linear three-dimensional effects on gravity-wave drag: Splitting flow and breaking waves. *Q. J. R. Met. Soc.* **118**, 1057–1082.

Rottman, J. W. & Smith, R. B. 1989 A laboratory model of severe downslope winds. *Tellus* **41A**, 401–415.

Taylor, J. 1992 The energetics of breaking events in a resonantly forced internal wave field. *J. Fluid Mech.* **239**, 309–340.

Thorpe, S. A. 1968*a* On standing internal gravity waves of finite amplitude. *J. Fluid Mech.* **32**, 489–528.

Thorpe, S. A. 1968*b* On the shape of progressive internal waves. *Phil. Trans. R. Soc. Lond.* A **263**, 563–614.

Thorpe, S. A. 1978*a* On the shape and breaking of finite-amplitude internal gravity waves in a shear flow. *J. Fluid Mech.* **85**, 7–31.

Thorpe, S. A. 1978*b* On internal gravity waves in an accelerating shear flow. *J. Fluid Mech.* **88**, 623–639.

Thorpe, S. A. 1981 An experimental study of critical layers. *J. Fluid Mech.* **103**, 321–344.

Thorpe, S. A. 1984 A laboratory study of stratified accelerating flow over a rough boundary. *J. Fluid Mech.* **138**, 185–196.

Thorpe, S. A. 1987 On the reflection of a train of finite-amplitude internal waves from a uniform slope. *J. Fluid Mech.* **178**, 279–302.

Thorpe, S. A. 1988 A note on breaking waves. *Proc. R. Soc. Lond.* A **419**, 323–335.

Thorpe, S. A. 1989 The distortion of short internal waves by a long wave, with application to ocean boundary mixing. *J. Fluid Mech.* **208**, 395–415.

Thorpe, S. A. 1994*a* The stability of statically unstable layers. *J. Fluid Mech.* **260**, 315–331.

Thorpe, S. A. 1994*b* Observations of parametric instability and breaking waves in an oscillating tilted tube. *J. Fluid Mech.* **261**, 33–45.

Winters, K. B. & D'Asaro, E. A. 1989 Two-dimensional instability of finite amplitude internal gravity wave packets near a critical layer. *J. Geophys. Res.* **94**, 12709–12719.

Winters, K. B. & Riley, J. J. 1992 Instability of internal waves near a critical level. *Dyn. Atmos. Oceans* **16**, 249–278.

Woods, J. D. 1968 Wave-induced shear instability in the seasonal thermocline. *J. Fluid Mech.* **32**, 791–800.

Wunsch, C. 1969 Progressive internal waves on slopes. *J. Fluid Mech.* **35**, 131–144.